CardioRenal Medicine

Cardiorenal Med 2017;7:234–244
DOI: 10.1159/000462984
Received: November 10, 2016
Accepted: February 1, 2017
Published online: May 24, 2017

Original Paper

Characterization of an Animal Model to Study Risk Factors and New Therapies for the Cardiorenal Syndrome, a Major Health Issue in Our Aging Population

Anja Verhulst Ellen Neven Patrick C. D'Haese

Laboratory of Pathophysiology, University of Antwerp, Antwerp, Belgium

Keywords
Cardiovascular disease · Anemia · Bone and mineral metabolism

Abstract
Background: The cardiorenal syndrome (CRS) is a major health problem in our aging population. The term was introduced to cover disorders of the kidneys and heart, whereby dysfunction of one organ may induce dysfunction of the other. As the natural history of the CRS is mostly slow, hence difficult to explore in clinical trials, adequate animal models combining cardiovascular and renal disease are required. Therefore, we developed and characterized a usable model for CRS type 4, i.e. chronic kidney disease (CKD) causing cardiac dysfunction. ***Methods:*** CKD was induced in rats by supplementing the diet with adenine. During 8 weeks, several aspects of CRS were studied: CKD, mineral-bone disorder (MBD), cardiovascular disease, and (iron-deficiency) anemia. Hereto, the following parameters were monitored: serum creatinine, calcium, phosphate, FGF23, dynamic bone parameters, aortic Ca deposits, heart weight, serum NT-proANP, Hct, Hb, reticulocytes, spleen iron, and serum hepcidin. ***Results:*** Animals developed a severe CKD together with a disturbed mineral balance as reflected by the increased serum creatinine and phosphorus levels and decreased serum calcium levels; and in association herewith aberrations in hormonal levels of FGF-23. In turn, the well-known and highly undesirable complications of CKD, i.e. high turnover bone disease and pathological vessel calcification were induced. Furthermore (iron-deficiency) anemia developed quickly. ***Conclusion:*** The animal model described in this article in many aspects mimics the human situation of the CRS type 4 and will be useful to concomitantly evaluate the effects of new treatment strategies on the various aspects of CRS.

Patrick C. D'Haese
University of Antwerp, CDE, Building T.0
Universiteitsplein 1
BE–2610 Antwerp (Belgium)
E-Mail patrick.dhaese@uantwerpen.be

Introduction

Maintenance of blood volume, vascular tone, and hemodynamic stability is controlled by a set of elegant interactions between the heart and kidney. For some time, physicians have recognized that severe dysfunction in either of these organs rarely occurs as an isolated event. However, only recently was the widespread concept of the cardiorenal syndrome (CRS) introduced and defined as a group of disorders of the heart and kidneys, whereby dysfunction of one organ induces or aggravates dysfunction of the other. Knowledge of the precise pathophysiological connections between the failing heart and kidneys is key in understanding the mechanisms underlying the CRS and would allow us to develop therapies that interrupt this dangerous feedback loop.

As the natural history of the CRS is mostly slow, hence difficult to explore in clinical trials, adequate animal models combining cardiovascular and renal disease are required to explore the physiopathological mechanisms, and even more importantly the development of new therapeutic targets. Therefore, we further developed and characterized our previously described model of CKD-MBD (chronic kidney disease – mineral and bone disorders) [1] and investigated whether it would be usable as a model for CRS type 4, as defined by the Ronco classification [2], i.e. CKD causing cardiac dysfunction.

CRS type 4 is a major health problem in our aging population. The prevalence of CKD steadily increases year by year [3], and CKD is associated with an increased risk for cardiovascular events and mortality in comparison with the general population [4]. Cardiovascular disease is even the most common cause of death in the setting of CKD, and individuals suffering from CKD stage 3 are more likely to die from cardiovascular disease than to develop end-stage renal disease [5].

In order to characterize the CKD-MBD rat model as a CRS type 4 model, we firstly evaluated the development of heart failure (hypertrophy). Furthermore, since a recent review article of Charytan et al. [5], next to abnormalities in the bone and mineral axis, also put forward abnormalities in iron metabolism and development of anemia as important factors in the pathogenesis and prevention or treatment of CRS, we also characterized these CKD-related complications in our animal model.

Materials and Methods

Study Setup and Mortality

Animals had free access to food and water and were housed 2 per cage. All animals were weighed weekly and monitored daily for morbidity.

Sixty male Wistar rats were used (225–250 g) and randomly assigned to different groups. The sample size of the different groups was determined by power analysis with respect to the 3R principle of animal ethics and expected mortality. An equilibration period of 3 weeks was included to ensure a body weight of approximately 320 g at the start of the study. CKD was induced by maintaining the rats (n = 56) on an adenine diet with low vitamin K (0.35% adenine, 0.2 mg/kg VitK, 1% Ca, 1% P, 1 IU/g VitD and 6% protein) (SSNIFF Spezialdiäten, Soest, Germany) for 4 subsequent weeks, followed by a diet with the same composition except for a relatively lower adenine concentration (0.25%) during the 4 following weeks. A control group (n = 4) with normal renal function was included and maintained on a control diet with low vitamin K (0.2 mg/kg VitK, 1% Ca, 1% P, 1 IU/g VitD and 6% protein). The CKD groups were sacrificed weekly starting from week 3 until week 8 (n = 8 for week 3 and 4, n = 10 for week 5, 6, 7, and 8), i.e. the end of the experiment. Animals that were fed a control diet were sacrificed at the end of the study (week 8, controls). Only 1 animal (from the 7 weeks group) died prior to planned sacrifice; consequently, n = 9 for all the results reported for this group.

Blood/Urine Sampling and Analyses

Every 2 weeks starting from week 0 until sacrifice, animals of the control group and the CKD group scheduled to be euthanized at week 8 were placed in individual metabolic cages for a 24-h urine collection, followed by blood sampling via the tail vein. The rats of the remaining groups were only put in metabolic cages for 24-h urine collection the day before sacrifice.

Urinary volume was recorded at the end of each collection. Two 5-mL aliquots of the urine collection were frozen at –20°C pending further analysis (Ca, P, creatinine, total protein). Blood samples were collected in Multivette 600 tubes by tail vein puncture in restrained, conscious animals or during exsanguination at sacrifice (±5 mL). After clotting on ice and centrifugation at high speed, two 250 µL aliquots of serum were stored at –20 and –80°C until further processing (Ca, P, creatinine, FGF-23, hepcidin, and N-terminal proatrial natriuretic peptide [NT-proANP]).

Labeling of the Bone

All animals received an i.p. injection of 30 mg/kg tetracycline and 25 mg/kg demeclocycline on day 7 and day 3 before sacrifice, respectively, for later histomorphometric analysis of a series of dynamic bone parameters (see below).

Sacrifice, Whole Blood Analysis, and Tissue Sampling

Animals were euthanized by exsanguination via the retro-orbital plexus after pentobarbital anesthesia (60 mg/kg i.p.). Whole blood analysis was performed immediately upon sampling using either i-STAT Point of Care technology (Abott point of care, Princeton, NJ, USA) for measuring hematocrit (Hct) and hemoglobin (Hb) concentrations or Sysmex technology (Sysmex corporation, Kobe, Japan) for quantification of the reticulocyte number and the mean corpuscular Hb (MCH) content (average Hb content/red blood cell).

Aorta, aa. carotis and femoralis, spleen, heart, and both tibiae were taken at sacrifice. The presence of vascular calcification was evaluated histomorphometrically on paraffin-embedded Von Kossa-stained sections of the thoracic aorta. Spleen and heart were weighted, and samples of the spleen were taken and preserved at –20°C pending measurement of iron. The left tibia was removed, cleared of soft tissue, and subsequently fixed in 70% ethanol and stored at 4°C until further processing for quantitative histomorphometric bone analysis.

Serum Analysis

Serum samples were analyzed for the following parameters: creatinine, calcium, phosphorus, FGF-23, hepcidin, and NT-proANP. Creatinine, phosphorus, hepcidin, FGF-23, and NT-proANP were measured using commercially available kits: Creatinine Merckotest (Diagnostica Merck, Darmstadt, Germany), Ecoline®S Phosphate (DiaSys, Holzheim, Germany), rat hepcidin Elisa (BioSource, San Diego, CA, USA), rat FGF-23 Elisa (Kainos, Tokyo, Japan), and rat NT-proANP (MesoScaleDiscovery, Rockville, MD, USA), respectively. Serum calcium was measured by flame atomic absorption spectrometry (FAAS, Perkin Elmer, Waltham, MA, USA).

Quantitative Histomorphometric Bone Analysis

The left tibia was cleared of soft tissue, and fixated overnight in 70% ethanol. After dehydration in increasing concentrations of alcohol, the samples were embedded in methylmetacrylate polymer. After polymerization, sections were cut using a heavy-duty microtome and mounted onto glass microscopy slides. Goldner-stained sections were used to quantify static bone parameters, while unstained sections were analyzed for the tetracycline labeling using fluorescence microscopy. All analyses are performed using an AxioVision v.4.5 image analysis system (Zeiss, Jena, Germany), running in-house developed programs. Out of the primary measured parameters, the following results were calculated and reported: osteoblast, osteoclast, and eroded perimeter (all three as percentage of total perimeter), mineral apposition rate (rate by which osteoid is mineralized, µm/day), bone formation rate (surface of bone formed per unit of time expressed per tissue area, $\mu m^2/mm^2$/day), and mineralization lag time (mean time interval between deposition and mineralization of osteoid days, days).

Iron Measurement in Spleen

After weighing, a piece of spleen tissue was homogenized with a tissue ruptor (Quiagen, Hilden, Germany) in 2 mL demineralized water, after which 2 mL HCl/TCA was added (HCl/TCA was prepared by adjusting 4 mL HCL [37%] to 50 mL with 10% TCA). Subsequently, the tissue homogenate was incubated for 1.5 h at 95°C and centrifuged for 10 min at 8,200 rcf. Finally, iron was measured by Zeeman corrected electrothermal atomic absorption spectrometry (Perkin Elmer, Waltham, MA, USA) in the supernatant [6].

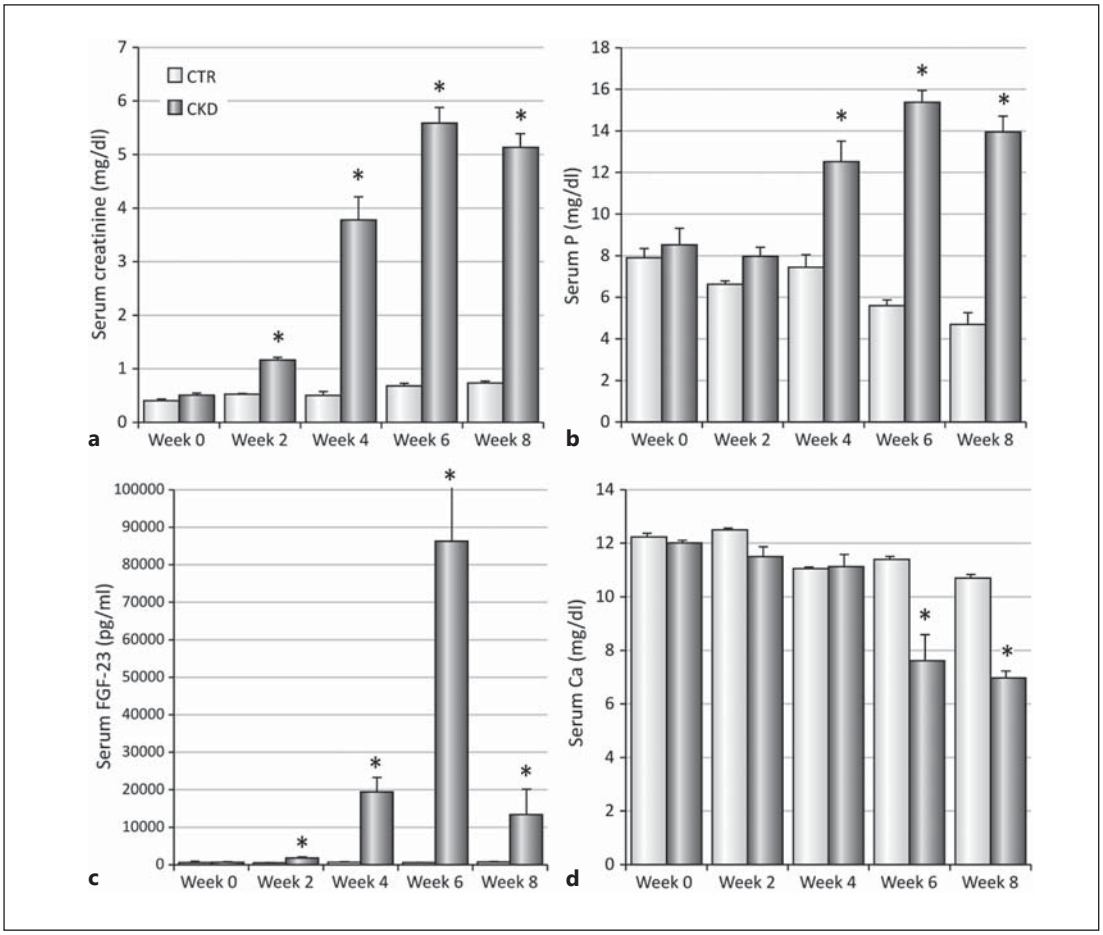

Fig. 1. Development of chronic kidney disease (CKD) (**a**) and disturbed mineral balance in serum (**b–d**) in animals receiving adenine-supplemented diet, compared to control (CTR) animals. **a** Serum creatinine. **b** Serum phosphate (P). **c** Serum FGF-23. **d** Serum calcium (Ca). Each data point represents mean ± SEM of 10 animals from the CKD group and 4 animals from the CTR group. * $p < 0.05$ vs. CTR.

Statistics

Results are expressed as mean ± SEM. Nonparametric statistical analyses were performed with SPSS 20.0 software (IBM Corp., Armonk, NY, USA). Statistical differences between groups were investigated with the Kruskal-Wallis test followed by the Mann-Whitney U test (two-tailed). Bonferroni correction was applied where appropriate. $p < 0.05$ is considered statistically significant.

Results

Mortality and Body Weight

Throughout the study, only one animal died prior to the scheduled sacrifice. Animals of the control group steadily gained weight, while body weight of CKD animals remained stable from the time point of adenine administration.

Development of CKD-MBD

Animals receiving the adenine-supplemented diet quickly developed impairment of renal function and disturbances of mineral balance (Fig. 1). The former was reflected by the

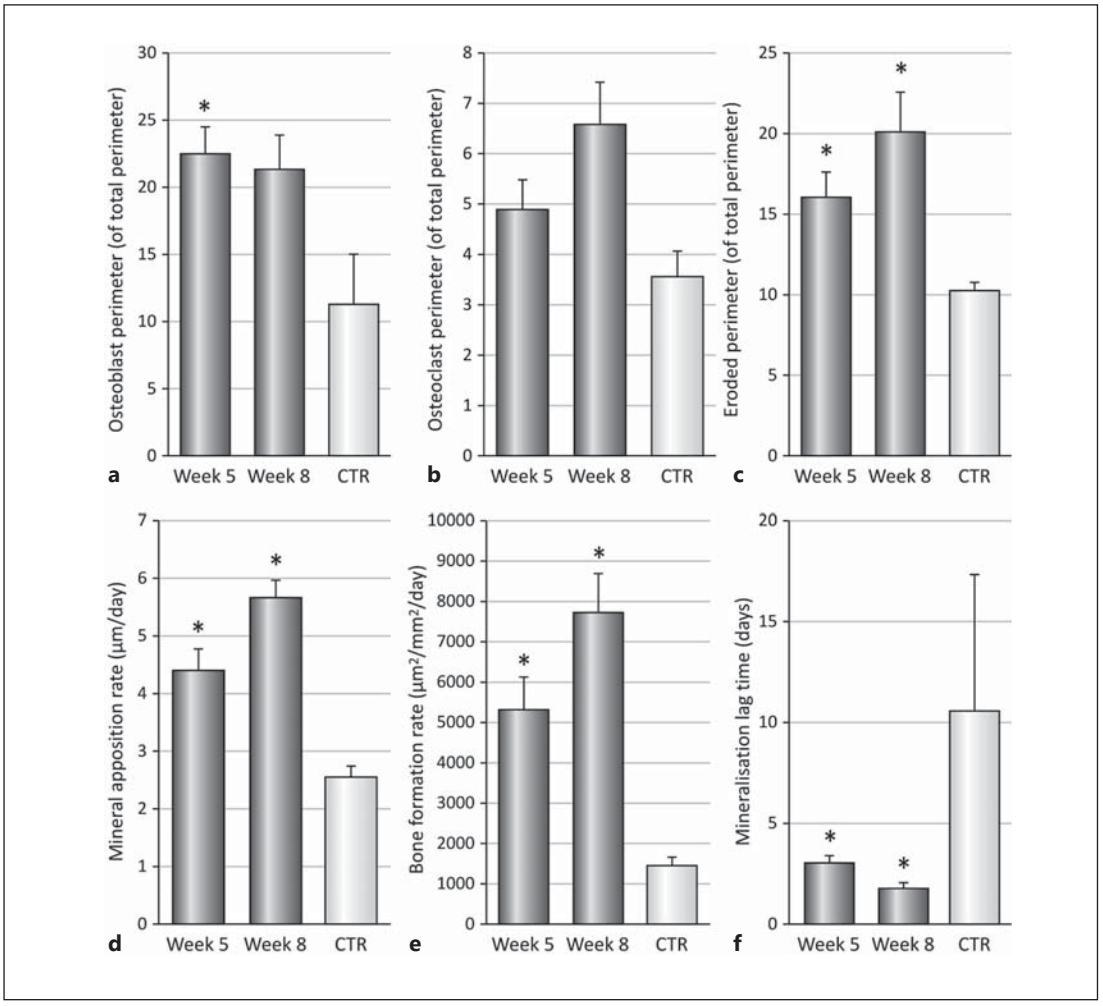

Fig. 2. Development of chronic kidney disease (CKD)-induced bone pathology (high-turnover bone disease) as became clear from measuring static (**a–c**) and dynamic (**d–f**) bone parameters in animals receiving an adenine-supplemented diet (CKD), compared to control (CTR) animals. **a** Osteoblast. **b** Osteoclast. **c** Eroded perimeter (all as percentage of total perimeter). **d** Mineral apposition rate. **e** Bone formation rate. **f** Mineralization lag time. Each data point represents mean ± SEM of 10 animals from the CKD week 5 and 8 groups, and of 4 animals from the CTR group. * $p < 0.05$ vs. CTR.

serum creatinine levels, which became significantly different from control values already at 2 weeks of adenine administration. After 6 weeks, a plateau was reached at concentrations almost 8 times higher than the control values (5.6 ± 0.03 vs. 0.7 ± 0.05 mg/dL). Concomitantly, the mineral balance of the animals was disturbed, as reflected by a significant hyperphosphatemia from week 4 on, reaching a triplication of control values at week 6 (15.4 ± 0.6 vs. 5.6 ± 0.3 mg/dL). Hyperphosphatemia was preceded by a significant rise in serum FGF-23 levels at week 2, achieving values that were 150 times higher than control values at week 6 (88,777 ± 33,945 vs. 583 ± 10 pg/mL). In line herewith, serum Ca concentrations significantly decreased from week 6 onwards (6.9 ± 0.3 vs. 10.7 ± 0.1 mg/dL at week 8).

As a result of the disrupted mineral balance, rats developed a disturbed bone and mineral metabolism. This well-known complication of CKD is mainly expressed as high turnover bone disease (Fig. 2) and concomitant arterial calcification (Fig. 3). High turnover bone disease was clearly observed from week 5 on as reflected by static (Fig. 2a–c) and dynamic bone param-

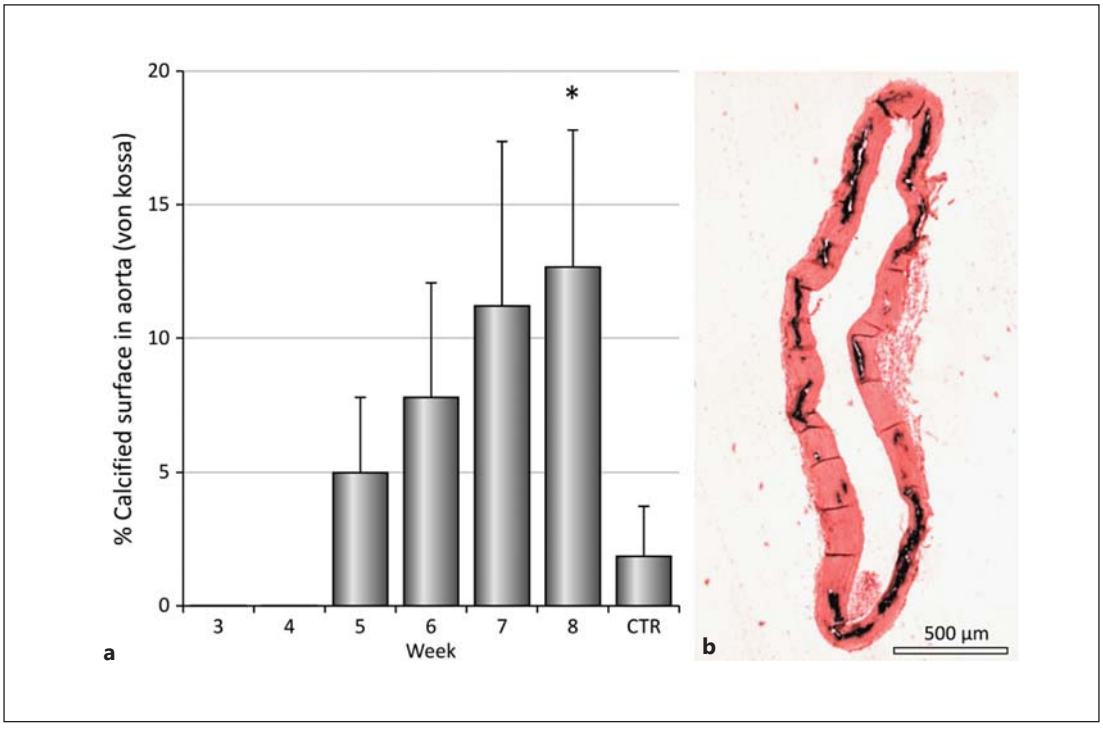

Fig. 3. Development of CKD-induced aortic calcifications in animals receiving adenine-supplemented diet, compared to control (CTR) animals. **a** Quantification of Von Kossa positive area percentage in tissue sections of CKD and CTR animals. Each data point represents mean ± SEM of 10 animals for the CKD week 5 and 8 groups and of 4 animals from the CTR group. * $p < 0.05$ vs. CTR. **b** Microscopic image of a Von Kossa-stained aortic section of an animal receiving adenine-supplemented diet (week 5, calcifications stain black).

eters (Fig. 2d–f). A significantly increased osteoblast (11 ± 4 to 22 ± 2%; Fig. 2a) and eroded (10 ± 0.5 to 16 ± 1.6%; Fig. 2c) perimeter were seen at week 5; osteoclast perimeter doubled (however not significant) from 10 ± 0.5 to 20 ± 2.5% at week 8 (Fig. 2b). Furthermore, at week 5 a significantly increased mineral apposition rate and bone formation rate and a significantly decreased mineralization lag time (Fig. 2d–f) were observed. These latter bone parameters worsened during the further course of the observation period resulting in a mineral apposition rate of 5.7 ± 0.4 µm/day (vs. controls 2.6 ± 0.2 µm/day), a bone formation rate of 7,722 ± 808 $\mu m^2/mm^2$/day (vs. controls 1,449 ± 213 $\mu m^2/mm^2$/day) and a mineralization lag time of 1.8 ± 0.4 days (vs. controls 10.6 ± 6 days) at week 8. Concomitantly with the high turnover bone disease at week 5, calcification in the aorta was detected (Fig. 3) as shown by Von Kossa positive staining of the aortic sections. After 8 weeks of CKD, the percent calcified surface in the aorta was significantly increased versus controls (12.7 ± 5.1 vs. 0.002 ± 0.0008% calcified surface).

CKD-Induced Iron-Deficiency Anemia

Hct and Hb values rapidly decreased in CKD (Fig. 4a, b): point of care analysis detected significant reductions in Hct and Hb after 3 weeks of CKD induction. Values further decreased steadily during the course of the study ending up with values as low as 22.9 ± 1.7% (vs. 47.3 ± 1.6% in controls) for Hct and 8.2 ± 0.3 g/dL (vs. 16.1 ± 0.5 g/dL in controls) for Hb. Whole blood analysis using Sysmex technology allowed us to count the amount of reticulocytes which at week 3 had almost halved to 0.16 ± 0.01 × 10^6/µL (vs. 0.3 ± 0.01 × 10^6/µL at baseline,

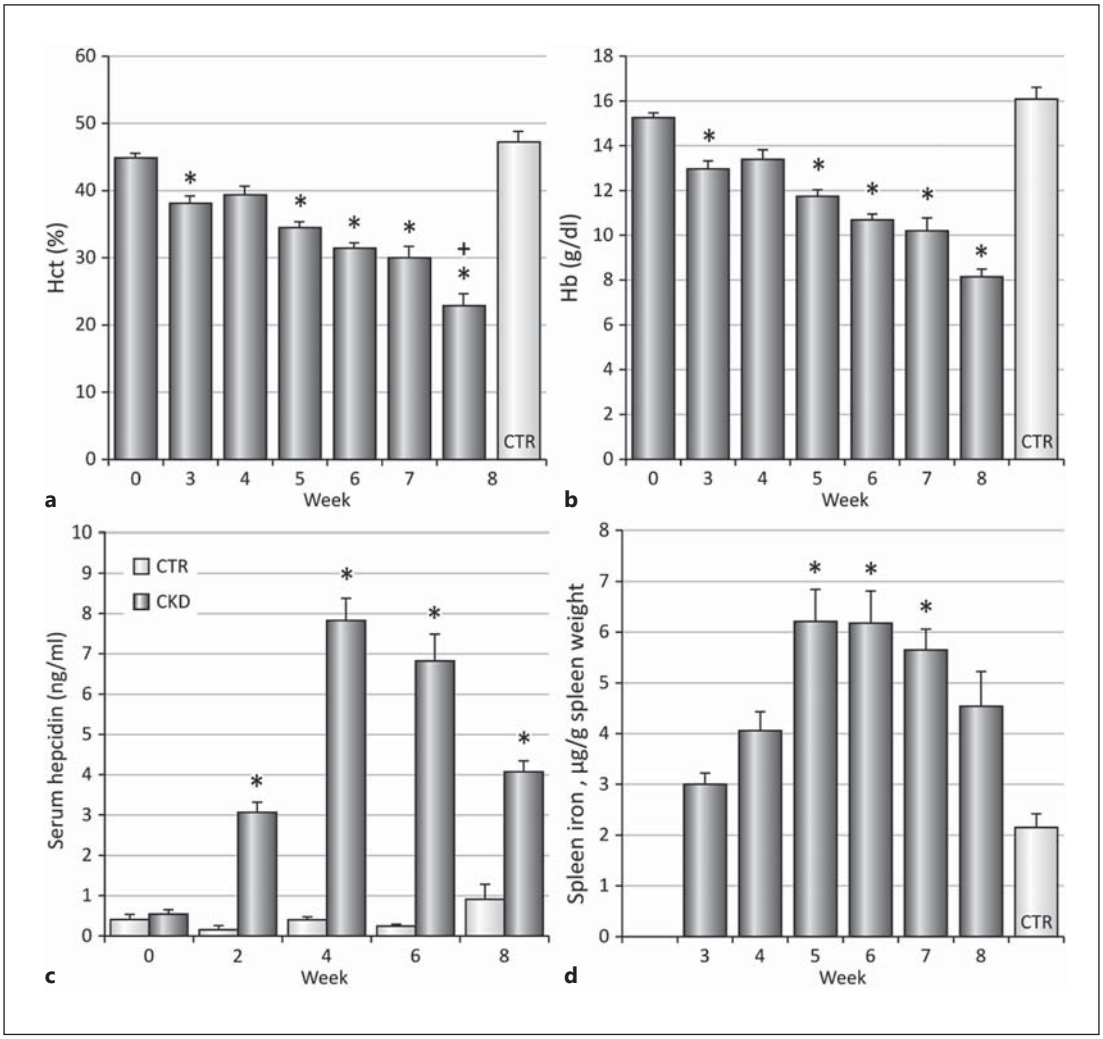

Fig. 4. Development of iron-deficiency anemia in animals receiving adenine-supplemented diet, compared to control (CTR) animals. **a** Whole-blood Hct levels. **b** Whole-blood Hb levels. **c** Serum hepcidin concentrations. **d** Spleen iron concentrations. **a**, **b**, **d** Each data point represents mean ± SEM of 8 animals from the CKD week 0, 3, and 4 groups, 9 animals from the CKD week 7 group, 10 animals from the CKD week 5, 6, and 8 groups, and 4 animals from the CTR group. **c** Each data point represents mean ± SEM of 10 animals from the CKD group and 4 animals from the CTR group. * $p < 0.05$ vs. CTR.

$p < 0.0005$), remaining constant at that low rate during the further course of the study. The amount of Hb in each erythrocyte or the MCH was decreased at week 3 (from 17.8 ± 0.15 to 16.8 ± 0.17 pg, $p = 0.005$) and remained constant during the further course of the study, except at week 8, where baseline values were reached again (17.2 ± 0.4 pg, $p = 0.17$ vs. baseline). Decreased MCH values indicate iron deficiency, further evidenced by 2 other critical parameters; i.e., serum hepcidin concentration and spleen iron concentration (Fig. 4c, d). Serum hepcidin became significantly increased already at week 2, attaining its highest level at week 4 reaching values almost as high as 20 times the average control level (7.8 ± 1.7 vs. 0.4 ± 0.1 ng/mL). Spleen iron levels, although measured at different time points, followed the same pattern: a significant increase at week 3, highest value at week 5 (2,085 ± 574 vs. 841 ± 218 µg/g wet weight), and partial normalization thereafter.

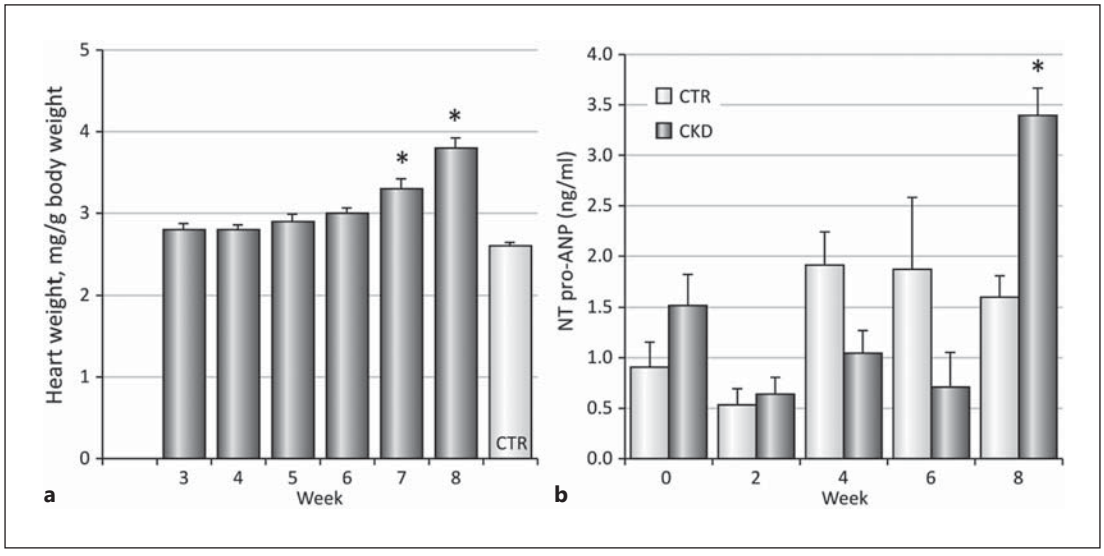

Fig. 5. Development of heart hypertrophy in animals receiving adenine-supplemented diet, compared to control (CTR) animals. **a** Heart weight (relative to body weight). Each data point represents mean ± SEM of 8 animals from the CKD week 3 and 4 groups, 9 animals from the CKD week 7 group, 10 animals from the CKD week 5, 6, and 8 groups, and 4 animals from the CTR group. **b** Serum N-terminal pro-ANP (NT-pro ANP) concentrations. Each data point represents mean ± SEM of 10 animals from the CKD group and 4 animals from the CTR group. * $p < 0.05$ vs. CTR.

Heart Failure

The development of heart failure or hypertrophy was reflected by the steadily increasing heart weight (normalized to body weight), which was significantly increased after 7 weeks of CKD and ended up with an almost 50% increase versus control values at the end of the study (Fig. 5a). Furthermore, the significantly increased serum NT-proANP concentration in CKD animals as compared to controls at week 8 (3.4 ± 0.8 vs. 1.6 ± 0.4 ng/mL) is in line with the development of heart hypertrophy (Fig. 5b).

Discussion

The animal model described in this article in many aspects mimics the human situation of CRS type 4. A severe CKD develops with the direct consequence of a disturbed mineral balance as reflected by the altered calcium and phosphorus levels and in association with the aberrations in hormonal levels of FGF-23 (PTH was not measured in this study but was reported earlier by our group to be increased in rats with adenine-induced CKD [1]) which in turn induced the well-known and highly undesirable complication of CKD, i.e. mineral and bone disorder (MBD) which is characterized by high turnover bone disease and pathological vessel calcification.

Furthermore, (iron-deficiency) anemia, another important CRS-associated comorbidity in humans [7], developed quickly. The increased serum hepcidin levels, together with proven iron retention in spleen, indicate that the anemia, at least partially, developed as a consequence of iron deficiency.

Although not yet fully understood, CKD patients often develop left ventricle hypertrophy ensuing in cardiac failure. The obvious hypertrophy of the heart together with the significant rise in NT-proANP, is indicative of a failing heart function in our animal model. Atrial natri-

uretic peptide is synthesized by cardiomyocytes in response to increased wall stress [8] and therefore is considered a valid marker for the assessment of heart failure and particularly of left ventricle hypertrophy/systolic dysfunction in humans [9, 10] and in rats [11]. Because the active peptide is rapidly degraded upon secretion, the concentrations of the NT-proANP better reflect the total amount of secreted atrial natriuretic peptide, both in humans and rats [12, 13].

To the best of our knowledge, this is the first report describing various characteristics/parameters used to diagnose CRS type 4 in humans in an animal model. The reciprocal interactions between all these parameters were extensively considered and discussed in the recent past, but remain only partially understood. In order to define the clinical manifestations of cardiovascular disease in patients with CKD, Silverberg et al. [14] proposed the term cardiorenal anemia syndrome (CRAS) to conceptualize the association between anemia and cardiorenal failure, and later on the term was even further refined to CRAIDS (cardiorenal anemia iron deficiency syndrome) by Klip et al. [15]. The term CKD-MBD was also introduced and is now frequently used to describe the relationship between CKD, abnormal mineral metabolism and vascular calcification; which has repeatedly been reported to importantly contribute to cardiovascular disease [16].

Less obvious interactions are the presumed direct promoting effect of FGF-23 on cardiomyocyte hypertrophy [17] and the anemia-independent worsening effect of iron deficiency on heart function [18]. Our results argue for an association between the bone mineral axis and iron metabolism. Indeed, for reasons that are not yet clear, at the end of the study, serum hepcidin, spleen iron, and serum FGF-23 concentrations together partially normalize. Hepcidin is a protein regulating iron homeostasis by blocking iron absorption from the gut and iron release from spleen macrophages [19]. Increased hepcidin levels are seen in states of iron overload or inflammation [20], in the latter case to deplete invading organisms from iron. Hepcidin levels are also elevated in CKD, and thus are thought to contribute to the dysregulation of iron homeostasis in patients with impaired renal function [21]. However, the primary factors associated with increased hepcidin levels in CKD patients are not fully understood. A study in CKD patients reported abnormalities in serum phosphate and FGF-23 levels to be associated with increased hepcidin levels independently of eGFR [22], suggesting a direct interaction between, on the one hand the phosphate metabolism, and on the other hand hepcidin and iron metabolism. In a more recent publication, the same authors provided experimental evidence for this interaction since iron deficiency stimulated FGF-23 production [23]. This interaction however does not explain why in the first place at the end of our study serum hepcidin, spleen iron, and serum FGF-23 partially normalize.

Testing new CRS treatment strategies in the animal model described in this article opens perspectives for more efficient treatment of CRS but can also importantly contribute to the elucidation of the reciprocal interactions between all CRS-related parameters, which in turn may initiate the development of more efficient and safer treatment strategies.

Treatments targeting iron deficiency have proven to be able to achieve satisfactory Hb levels without the administration of erythropoietin-stimulating agents as in clinical studies intravenous iron administration resulted in a substantial increase in the Hb level [24]. Administration of a molecule antagonizing hepcidin function in a CKD rat model was able to reverse anemia [25]. Furthermore, those treatments possibly should also affect cardiac function: intravenous administration of ferric carboxymaltose in a clinical study improved symptoms of heart failure [26]. The current animal model will allow us to investigate in a straightforward manner whether treatments targeting iron deficiency, in addition to anemia, are also able to improve other CKD-induced comorbidities such as MBD, which in view of the above-mentioned link between phosphate metabolism and iron deficiency is worth being considered.

Treatment of the most fatal complication of CKD, i.e. vascular calcification, until now has not been proven highly efficacious and in general is limited to optimizing the mineral metab-

olism and related bone disease, e.g. by using phosphate binders, to which it is inextricably linked. An alternative approach could be to directly interfere with the calcification process by for example treatment with the endogenic calcification inhibitor pyrophosphate either or not in combination with its most important degrading enzyme tissue nonspecific alkaline phosphatase. Another therapeutic strategy could consist in the therapeutic use of ferric pyrophosphate (Fe-PPi or Triferic) [27] which would allow us to directly evaluate the combined effect of this treatment on vascular calcification and iron-deficiency-related anemia in one and the same animal. As such, our current model again would enable to test the effects of these particular treatments on all aspects of the CRS.

Another new treatment strategy in the setting of CKD-MBD/CRS consists in the use of the activin receptor IIA ligand trap which, based on its characteristics, might exert a beneficial effect on the most important CKD complications: anemia, bone disease, and vascular calcification. Activin receptor IIA ligand trap has proven to have beneficial effects in different models of anemia (including hepcidin transgenic mice) and bone loss [28–31]; however, so far it has never been tested in the setting of CKD-induced anemia and bone mineral disorder. In a recent article, however, it has been elegantly shown to prevent aortic intima calcification and even decrease renal fibrosis in an LDL receptor knockout model [32].

Acknowledgements

We generously thank Rita Marynissen, Hilde Geryl, Geert Dams, and Ludwig Lamberts for their tremendous assistance in animal care and/or laboratory work. We want to thank Dirk De Weerdt for support with the graphical work of this article. Anja Verhulst was and Ellen Neven still is a postdoctoral fellow of the Fund for Scientific Research Flanders (26121 to A.V. and 31821 to E.N.).

Statement of Ethics

Experimental procedures were conducted according to the National Institutes of Health Guide for the Care and Use of Laboratory Animals (1996) and were approved by the University of Antwerp Ethical Committee.

Disclosure Statement

The authors declare that they do not have any conflict of interest.

References

1 Neven E, Bashir-Dar R, Dams G, Behets GJ, Verhulst A, Elseviers M, D'Haese PC: Disturbances in bone largely predict aortic calcification in an alternative rat model developed to study both vascular and bone pathology in chronic kidney disease. J Bone Miner Res 2015;30:2313–2324.
2 Ronco C, Haapio M, House AA, Anavekar N, Bellomo R: Cardiorenal syndrome. J Am Coll Cardiol 2008;52:1527–1539.
3 NIH: NIH Kidney disease statistics for the US. 2010. http://www.niddk.nih.gov/health-information/health-statistics/Documents/KU_Diseases_Stats_508.pdf.
4 Sarnak MJ, Levey AS, Schoolwerth AC, Coresh J, Culleton B, Hamm LL, McCullough PA, Kasiske BL, Kelepouris E, Klag MJ, Parfrey P, Pfeffer M, Raij L, Spinosa DJ, Wilson PW: Kidney disease as a risk factor for development of cardiovascular disease: a statement from the American Heart Association Councils on Kidney in Cardiovascular Disease, High Blood Pressure Research, Clinical Cardiology, and Epidemiology and Prevention. Hypertension 2003;42:1050–1065.
5 Charytan DM, Fishbane S, Malyszko J, McCullough PA, Goldsmith D: Cardiorenal syndrome and the role of the bone-mineral axis and anemia. Am J Kidney Dis 2015;66:196–205.
6 Liang L, D'Haese PC, Lamberts LV, De Broe ME: Direct determination of iron in urine and serum using graphite furnace atomic absorption spectrometry. Analyst 1989;114:143–147.

7 Jankowska EA, von Haehling S, Anker SD, Macdougall IC, Ponikowski P: Iron deficiency and heart failure: diagnostic dilemmas and therapeutic perspectives. Eur Heart J 2013;34:816–829.
8 Levin ER, Gardner DG, Samson WK: Natriuretic peptides. N Engl J Med 1998;339:321–328.
9 Jortani SA, Prabhu SD, Valdes R Jr: Strategies for developing biomarkers of heart failure. Clin Chem 2004;50:265–278.
10 Muders F, Kromer EP, Griese DP, Pfeifer M, Hense HW, Riegger GA, Elsner D: Evaluation of plasma natriuretic peptides as markers for left ventricular dysfunction. Am Heart J 1997;134:442–449.
11 Crivellente F, Bocchini N, Bonato M, Vandin L, Faustinelli I, Cristofori P: Atrial natriuretic peptides in Han Wistar, Sprague-Dawley and spontaneously hypertensive rats. J Appl Toxicol 2012;32:521–526.
12 McDowell G, Patterson C, Maguire S, Shaw C, Nicholls DP, Hall C: Variability of Nt-proANP and C-ANP. Eur J Clin Invest 2002;32:545–548.
13 Thibault G, Murthy KK, Gutkowska J, Seidah NG, Lazure C, Chretien M, Cantin M: NH2-terminal fragment of rat pro-atrial natriuretic factor in the circulation: identification, radioimmunoassay and half-life. Peptides 1988;9:47–53.
14 Silverberg DS, Wexler D, Blum M, Iaina A: The cardiorenal anemia syndrome: correcting anemia in patients with resistant congestive heart failure can improve both cardiac and renal function and reduce hospitalizations. Clin Nephrol 2003;60(suppl 1):S93–S102.
15 Klip IT, Jankowska EA, Enjuanes C, Voors AA, Banasiak W, Bruguera J, Rozentryt P, Polonski L, van Veldhuisen DJ, Ponikowski P, Comin-Colet J, van der Meer P: The additive burden of iron deficiency in the cardiorenal-anaemia axis: scope of a problem and its consequences. Eur J Heart Fail 2014;16:655–662.
16 KDIGO: KDIGO clinical practice guideline for the diagnosis, evaluation, prevention, and treatment of Chronic Kidney Disease-Mineral and Bone Disorder (CKD-MBD). Kidney Int Suppl 2009;113:S1–S130.
17 Faul C, Amaral AP, Oskouei B, Hu MC, Sloan A, Isakova T, Gutierrez OM, Aguillon-Prada R, Lincoln J, Hare JM, Mundel P, Morales A, Scialla J, Fischer M, Soliman EZ, Chen J, Go AS, Rosas SE, Nessel L, Townsend RR, Feldman HI, St John Sutton M, Ojo A, Gadegbeku C, Di Marco GS, Reuter S, Kentrup D, Tiemann K, Brand M, Hill JA, Moe OW, Kuro OM, Kusek JW, Keane MG, Wolf M: FGF23 induces left ventricular hypertrophy. J Clin Invest 2011;121:4393–4408.
18 Comin-Colet J, Enjuanes C, Gonzalez G, Torrens A, Cladellas M, Merono O, Ribas N, Ruiz S, Gomez M, Verdu JM, Bruguera J: Iron deficiency is a key determinant of health-related quality of life in patients with chronic heart failure regardless of anaemia status. Eur J Heart Fail 2013;15:1164–1172.
19 Ganz T, Nemeth E: Hepcidin and iron homeostasis. Biochim Biophys Acta 2012;1823:1434–1443.
20 Drakesmith H, Prentice AM: Hepcidin and the iron-infection axis. Science 2012;338:768–772.
21 Babitt JL, Lin HY: Mechanisms of anemia in CKD. J Am Soc Nephrol 2012;23:1631–1634.
22 Carvalho C, Isakova T, Collerone G, Olbina G, Wolf M, Westerman M, Gutierrez OM: Hepcidin and disordered mineral metabolism in chronic kidney disease. Clin Nephrol 2011;76:90–98.
23 David V, Martin A, Isakova T, Spaulding C, Qi L, Ramirez V, Zumbrennen-Bullough KB, Sun CC, Lin HY, Babitt JL, Wolf M: Inflammation and functional iron deficiency regulate fibroblast growth factor 23 production. Kidney Int 2016;89:135–146.
24 Ben-Assa E, Shacham Y, Shashar M, Leshem-Rubinow E, Gal-Oz A, Schwartz IF, Schwartz D, Silverberg DS, Chernin G: Target hemoglobin may be achieved with intravenous iron alone in anemic patients with cardiorenal syndrome: an observational study. Cardiorenal Med 2015;5:246–253.
25 Sun CC, Vaja V, Chen S, Theurl I, Stepanek A, Brown DE, Cappellini MD, Weiss G, Hong CC, Lin HY, Babitt JL: A hepcidin lowering agent mobilizes iron for incorporation into red blood cells in an adenine-induced kidney disease model of anemia in rats. Nephrol Dial Transplant 2013;28:1733–1743.
26 Anker SD, Comin Colet J, Filippatos G, Willenheimer R, Dickstein K, Drexler H, Luscher TF, Bart B, Banasiak W, Niegowska J, Kirwan BA, Mori C, von Eisenhart Rothe B, Pocock SJ, Poole-Wilson PA, Ponikowski P: Ferric carboxymaltose in patients with heart failure and iron deficiency. N Engl J Med 2009;361:2436–2448.
27 Gupta A, Lin V, Guss C, Pratt R, Ikizler TA, Besarab A: Ferric pyrophosphate citrate administered via dialysate reduces erythropoiesis-stimulating agent use and maintains hemoglobin in hemodialysis patients. Kidney Int 2015;88:1187–1194.
28 Langdon JM, Barkataki S, Berger AE, Cheadle C, Xue QL, Sung V, Roy CN: RAP-011, an activin receptor ligand trap, increases hemoglobin concentration in hepcidin transgenic mice. Am J Hematol 2015;90:8–14.
29 Fields SZ, Parshad S, Anne M, Raftopoulos H, Alexander MJ, Sherman ML, Laadem A, Sung V, Terpos E: Activin receptor antagonists for cancer-related anemia and bone disease. Expert Opin Investig Drugs 2013;22:87–101.
30 Dussiot M, Maciel TT, Fricot A, Chartier C, Negre O, Veiga J, Grapton D, Paubelle E, Payen E, Beuzard Y, Leboulch P, Ribeil JA, Arlet JB, Cote F, Courtois G, Ginzburg YZ, Daniel TO, Chopra R, Sung V, Hermine O, Moura IC: An activin receptor IIA ligand trap corrects ineffective erythropoiesis in beta-thalassemia. Nat Med 2014;20:398–407.
31 Raje N, Vallet S: Sotatercept, a soluble activin receptor type 2A IgG-Fc fusion protein for the treatment of anemia and bone loss. Curr Opin Mol Ther 2010;12:586–597.
32 Agapova OA, Fang Y, Sugatani T, Seifert ME, Hruska KA: Ligand trap for the activin type IIA receptor protects against vascular disease and renal fibrosis in mice with chronic kidney disease. Kidney Int 2016;89:1231–1243.